Australian Journal of Earth Sciences: An International Geoscience Journal of the Geological Society of Australia
Publication details, including instructions for authors and subscription information:
http://www.tandfonline.com/loi/taje20

3-D structure of the Australian lithosphere from evolving seismic datasets

S. Fishwick [a] & N. Rawlinson [b]

[a] Department of Geology, University of Leicester, University Road, Leicester, LE1 7RH, UK

[b] Research School of Earth Sciences, The Australian National University, Canberra, ACT, 0200, Australia

Version of record first published: 30 Jul 2012

To cite this article: S. Fishwick & N. Rawlinson (2012): 3-D structure of the Australian lithosphere from evolving seismic datasets, Australian Journal of Earth Sciences: An International Geoscience Journal of the Geological Society of Australia, 59:6, 809-826

To link to this article: http://dx.doi.org/10.1080/08120099.2012.702319

Australian Journal of Earth Sciences (2012) **59**, (809–826)

3-D structure of the Australian lithosphere from evolving seismic datasets

S. FISHWICK[1]* AND N. RAWLINSON[2]

[1]*Department of Geology, University of Leicester, University Road, Leicester LE1 7RH, UK.*
[2]*Research School of Earth Sciences, The Australian National University, Canberra, ACT 0200, Australia.*

During the last 20 years, seismic tomography has frequently been used to provide information on the structure of the lithosphere beneath the Australian continent. New tomographic models are presented using two complementary seismological techniques in order to illustrate the current state-of-knowledge. Surface wave tomography is the ideal method to obtain information of velocity variations across the whole continent. The latest models use data from over 13 000 source–receiver paths, allowing a higher resolution than in previous studies using the same technique. In Western Australia the results at 100 km depth clearly reveal the contrast in structure between the Pilbara and Yilgarn Cratons and the Capricorn Orogen. At greater depths, the Kimberley Block has a distinct fast velocity anomaly in comparison with the surrounding mobile belts. In the east of the continent, strong horizontal gradients in velocity indicate transitions in lithospheric structure, although the new high resolution models reveal a complexity in the transitions through central Victoria and New South Wales. Complementing the surface wave tomography, we also present the results from the inversion of over 25 000 relative arrival times from body wave phases recorded in southeast Australia and Tasmania. The body wave tomography uses the surface wave model to provide information on long-wavelength structure and absolute velocities that would otherwise be lost. The new results indicate a distinct boundary between the Delamerian and Lachlan orogens within the upper mantle, the location of which is consistent with an east-dipping Moyston Fault, as observed by deep seismic reflection profiling. The new models also confirm a distinct region of fast velocities beneath the central sub province of the Lachlan Orogen. A significant new observation is that the inferred eastern edge of this central sub-province has a strong correlation with the location of copper/gold deposits; a similar relationship is observed at a larger scale in Western Australia where mineral deposits appear to flank the regions of fastest velocity within the West Australian Craton.

KEY WORDS: tomography, mantle, lithosphere, body waves, surface waves, cratons.

INTRODUCTION

The geology of Australia (Figure 1) records a history from the early Archean through to the present day (e.g. Betts *et al.* 2002). In order to understand the tectonic evolution of the continent over such a long period, observations from the surface are not sufficient, and we require approaches that allow us to image both the crustal structure and the properties of the underlying mantle. While a range of geophysical techniques have been used for this class of sub-surface imaging, seismic tomography offers the best approach for investigating regional-to-continental scale variations in the properties of the upper mantle. However, the results from tomographic studies do not remain static. As both techniques and datasets evolve, so to do the resulting models of upper mantle structure. This evolution of models can make interpretations somewhat frustrating, but is a natural aspect of tomographic studies—data coverage is never complete, and new data can always add new information. Ideally, as data are added, the changes in appearance of the tomographic model will be evolutionary rather than revolutionary, which can thus give confidence in key features. Additionally as new techniques are developed, such as full waveform tomography, the models should represent Earth structure even more realistically.

The focus of this manuscript is to present updated surface wave and body wave tomography results for the Australian continent, in the context of the evolutionary progression of seismic tomography models over the last two decades.

Previous Studies

A variety of seismological techniques have been performed on data in order to recover the seismic velocity structure in the crust and upper mantle beneath the Australian continent (see e.g. Kennett 2003). Point information can be obtained for the crust and upper mantle from receiver function studies (e.g. Reading *et al.* 2007; Ford *et al.* 2010) and in northern Australia body

*Corresponding author: sf130@le.ac.uk

ISSN 0812-0099 print/ISSN 1440-0952 online
http://dx.doi.org/10.1080/08120099.2012.702319

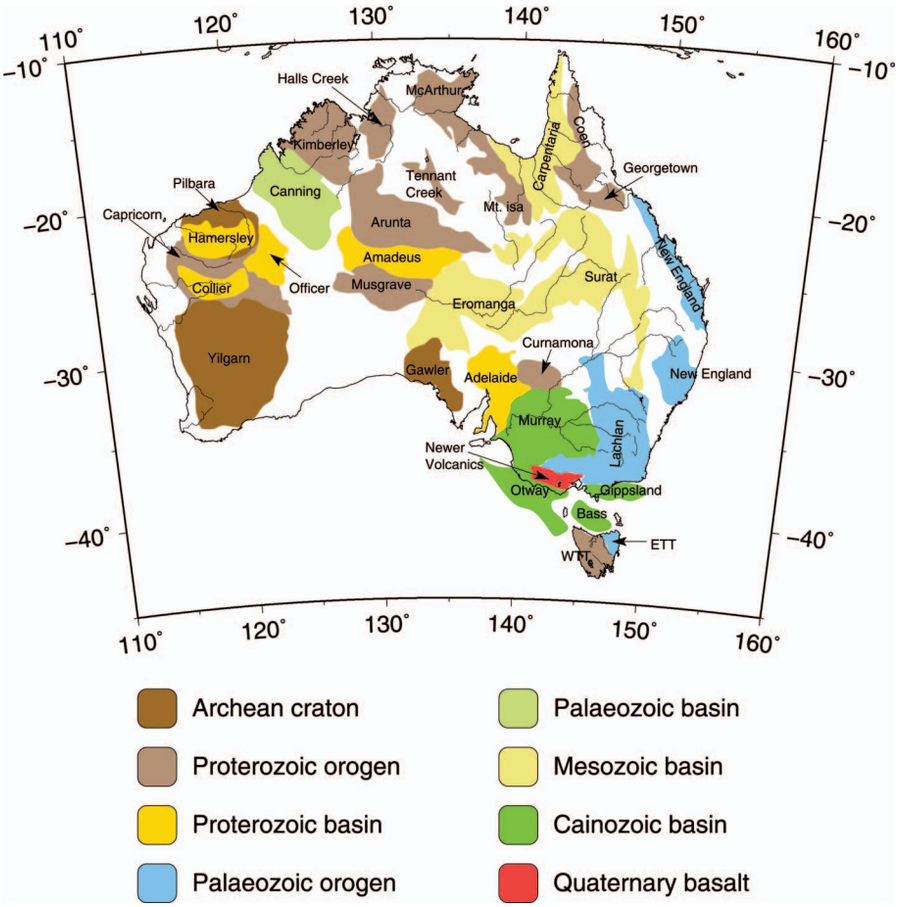

Figure 1 Map showing the large-scale geological features of the Australian continent.

wave information has been exploited to produce pseudo-3D models of the velocity variation (e.g. Kaiho & Kennett 2000). In this summary, we focus on the results from tomographic studies that have been used to construct velocity models of the upper mantle.

SURFACE WAVE TOMOGRAPHY

Owing to the location of seismic sources surrounding the continent, and the temporary deployments of broad-band seismometers—beginning with the SKIPPY experiment in the mid 1990s (van der Hilst *et al.* 1994)—which give continent-wide coverage of seismic stations, surface wave tomography has been frequently used to provide information at the continental-scale (Figure 2). The majority of studies have used either a methodology based on partitioned waveform inversion of the whole seismogram (e.g. Zielhuis & van der Hilst 1996; Simons *et al.* 1999, 2002) or a technique using secondary observables derived from the seismogram within the waveform inversion process (e.g. Debayle 1999; Debayle & Kennett 2000; Yoshizawa & Kennett 2004; Fishwick *et al.* 2005, 2008; Fishwick & Reading 2008). Both of these approaches first calculate a 1D velocity model to approximate the average velocity structure between source and receiver. The full set of 1D models is then combined within a tomographic inversion scheme to reconstruct the regional velocity variations.

Alternative approaches to surface wave tomography can be applied. Measurements of phase velocity may be related directly to shear velocity structure within a single inversion (e.g. Boschi & Ekström 2002; Schäfer *et al.* 2011); however, this technique has not been applied at a regional scale for Australia. Recently, Fichtner *et al.* (2009, 2010) developed a method of full waveform tomography, which uses spectral element simulations of seismic wave propagation in combination with adjoint techniques to construct a model of the 3D velocity variations. The advantage of full waveform tomography is that the waveforms are matched based on the correct solution of the equations of motion in a heterogeneous earth, and artefacts owing to simplifications of the wave propagation are avoided (Fichtner *et al.* 2009). However, the computational demands of this approach, means that in comparison with models using approximations of wave propagation, less data can be included in the inversion. This makes comparisons between different approaches very difficult; while resolution is predominately determined by data coverage and quality, resulting models should be more realistic with the inclusion of the correct solution of the equations of motion (Fichtner *et al.* 2009).

The surface wave studies described above have all revealed a number of features in the upper mantle related to the tectonic evolution of the Australian continent. It has long been recognised that there is a significant difference in sub-surface structure between the Precambrian shield region of western and central Australia and the younger Phanerozoic terranes in the east (Figure 1). Travel times from nuclear explosions

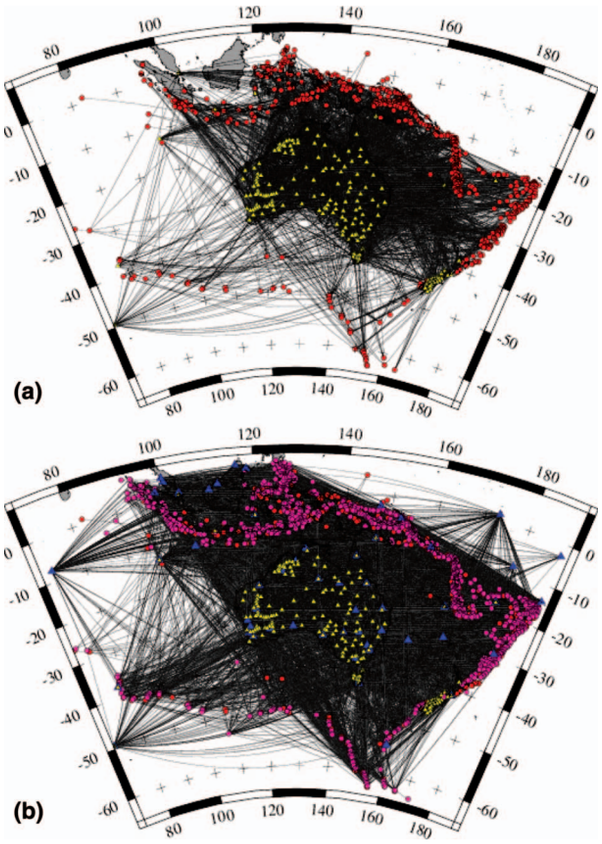

Figure 2 Map showing the path coverage, earthquake sources and seismometers used in the surface wave studies. (a) Fishwick *et al.* (2008) and (b) the present study. Earthquakes from the earlier study are in red, while locations of additional epicentres used in the present study are in purple. Similarly, the original networks of seismometers used are shown as yellow triangles, the location of additional seismometers used in the present study are shown as slightly larger blue triangles.

indicate fast anomalies within the shield areas, and slow wavespeeds in southeast Australia and Tasmania (Cleary 1967). The surface wave model of Simons *et al.* (2002) has been used to investigate whether there is any age-dependence of the fast velocities in the shield region. Defining a vertical extent of the seismic lithosphere by the +1% velocity contour, Simons & van der Hilst (2002) found that at scale lengths of less than 1000 km, the relationship between the age of the overlying geology and the lithospheric thickness is more complicated than had been suggested by global studies. The potential economic importance of our understanding of the location of cratonic lithosphere, has been illustrated by Jaques & Milligan (2004) and O'Neill *et al.* (2005) in relation to the location of kimberlite deposits that appear to be found close to the edge of regions of thicker lithosphere. Additionally, Begg *et al.* (2010) also found that many worldwide Ni–Cu–PGE sulfide deposits lie in close proximity to the boundaries of cratonic blocks.

Within the Yilgarn Craton, the results from the surface wave tomography of Fishwick *et al.* (2005) have been integrated alongside seismic reflection and refraction data, and receiver functions to construct a 3D geological/seismic model of the region (Goleby *et al.* 2006). This style of 3D model can yield important information on features such as crustal shear zones—related to mineral rich regions, and the inclusion of the passive-source seismic results can indicate whether terrane boundaries at the surface extend into the lithospheric mantle. Further analysis of the lithospheric architecture of this region, and the associated relevance to gold mineralisation, have included information from the tomographic study. While this analysis includes a wide range of geophysical, stratigraphic and geochemical information, the main emphasis from surface wave studies has been placed on the location of a high ($Vs > 4.8$ km/s) wavespeed body, and the variation in depth as to where this occurs (see e.g. Blewett *et al.* 2010; Czarnota *et al.* 2010).

The nature of the transition from the cratonic blocks, which make up the Precambrian shield region of central and western Australia, to the Phanerozoic terranes in the east (Figure 1) is another question that has been addressed. Direen & Crawford (2003) discussed the concept of the Tasman Line, and whether the interpretation of magnetic and gravity lineaments could be attributed to a single event—the breakup of Rodinia. The authors suggested that the idea of a single line was misleading, and that the protracted geological history from the Neoproterozoic to the Carboniferous gives rise to a variety of geophysical responses (Direen & Crawford 2003). Following this work, Kennett *et al.* (2004a) described the results from a range of seismic studies in order to provide information on the nature of this transition in the mantle. The results suggested that there was not a simple relationship between the location of transitions in mantle properties and the lineaments defined at the surface. As the datasets, and models, evolved, a more detailed analysis of the surface wave tomography was undertaken highlighting a number of 'steps' in the upper mantle velocity structure. These features were associated with variations in lithospheric thickness beneath provinces of different ages (Fishwick *et al.* 2008).

The easternmost step in lithospheric structure marks a strong gradient in wavespeed inland of the continent–ocean transition (Fishwick *et al.* 2008). The very slow velocities on the eastern margin of the continent were recognised in the early surface wave study of Zielhuis & van der Hilst (1996), and have since remained an integral part of all the tomographic models. However, despite all surface wave models showing slow wavespeeds in this region, at scale lengths of less than 500 km the location of the strongest velocity anomalies remains very variable between three recent models (see Fichtner *et al.* 2012). There is a broad correlation between the location of the slow wavespeeds and the location of Cenozoic volcanism along the east coast and in southern Australia. It is plausible that a pre-existing lithospheric structure may have controlled the location of the volcanism. In southern Australia, the rapid change in lithospheric thickness has been proposed as a driver for edge-driven convection, which manifests at the surface as the Newer Volcanics province (Demidjuk *et al.* 2007).

One of the fundamental limitations of surface wave tomography is the lateral resolution of the technique. Owing to the periods used to image structures in the upper mantle, even in areas with an excellent distribution of stations and good azimuthal variation in path coverage, the optimum horizontal resolution is likely to be approximately 100–200 km. In order to provide more detailed models, body waves need to be included in the analysis.

BODY WAVE TOMOGRAPHY

Owing to the sub-vertical propagation paths of body waves from distant earthquakes, and the sparse station distribution, continental-scale body wave tomography of the upper mantle beneath Australia has received less attention than the continental-scale surface wave tomography. However, the proximity of the Indonesian subduction zones, has allowed first order variations in structure on the northern margin of the continent to be highlighted in work focusing on the nature of the subducted slabs (e.g. Widiyantoro & van der Hilst 1996). Gorbatov & Kennett (2003) also produced models of bulk-sound speed and shear wavespeed variations, from the joint inversion of P and S wave arrival times. These models were predominately used to investigate variations in structure within the subduction zones, with the results for the Australian region presented by Kennett (2003) and Kennett *et al.* (2004b). The joint tomography results indicate that the transition from fast to slow wavespeeds associated with the Tasman Line is particularly strong for shear wavespeed, but not as apparent in the bulk-sound speed. Within the Yilgarn and Pilbara Cratons there is also significant small-scale variation in shear wavespeed; results that are compatible with the type of features observed in the surface wave models. More recently, Kennett & Abdullah (2011) presented results from an attenuation study of the Australian continent. Although this includes more data than the earlier body wave studies, the nature of the parameterisation (and focus of the study on attenuation) means that the velocity structure is not recovered at the same resolution as the earlier work.

In contrast to the results at the continental scale, within southeast Australia body wave tomography has been used to elucidate relatively detailed structure. This has been made possible by the initiation of a different class of passive seismic experiment in the late 1990s. The first of these involved an array of 40 short-period recorders that were deployed in western Victoria in 1998 with a station spacing of only 50 km, which allowed finer-scale features such as the Moyston Fault and the hot spot beneath the Newer Volcanics province to be illuminated (Graeber *et al.* 2002). This array was then moved twice in the subsequent two years to achieve contiguous coverage of the southwest Lachlan Orogen and Adelaide Fold Belt (Clifford *et al.* 2008).

These first three high-density passive array deployments in southeast Australia represent the beginnings of what is now known as the WOMBAT project (Rawlinson *et al.* 2011), which involves the use of a transportable array of instruments to achieve high-density passive seismic coverage of southeast Australia. To date, there have been 15 array deployments throughout Tasmania, Victoria, New South Wales and southern South Australia that have resulted in a total of nearly 600 site locations with interstation spacings of 50 km on the mainland and 15 km in Tasmania (see Figure 3). Typically, each array is deployed for a period of 6–12 months before it is moved to a new location.

The natural seismicity recorded by the WOMBAT arrays include P and S body waves from distant earthquakes, ambient noise from oceanic microseisms and atmospheric disturbances, and local earthquakes. In the latter case, the recording duration is generally not sufficient to record enough events in the vicinity of the array to usefully contribute to seismic imaging. The principal technique used so far to image lithospheric structure is teleseismic tomography, which exploits the relative arrival times of distant earthquakes across an array in order to recover lateral variations in velocity throughout a 3-D volume beneath the array (see Rawlinson *et al.* 2010b for a review of the technique). A number of studies have been carried out on data recorded by individual arrays (Graeber *et al.* 2002; Rawlinson *et al.* 2006a, b; Rawlinson & Urvoy 2006; Clifford *et al.* 2008; Rawlinson & Kennett 2008), but recent efforts have focused on trying to combine data from multiple arrays in order to generate unified models of larger regions (Rawlinson *et al.* 2010a, 2011). The results of these teleseismic tomography studies have yielded new information on the structure and tectonic evolution of southeast Australia. For instance, Graeber *et al.* (2002) find that there is a $\sim 2\%$ increase in P-wave velocity across the Moyston Fault Zone from east to west, and conclude that it represents a major lithospheric boundary. Graeber *et al.* (2002) also find pronounced low velocities beneath the eastern part of the Newer Volcanics province and suggest that these results from reduced mantle velocities associated with a hot-spot-related high temperature anomaly.

As the WOMBAT experiment has grown, more recent teleseismic tomography results have expanded on the early findings of Graeber *et al.* (2002). Rawlinson *et al.* (2011) find that the velocity contrast across the Moyston Fault Zone extends northwards into New South Wales, and interpret it to be the boundary between Proterozoic and Paleozoic lithosphere extending beneath the Western Subprovince of the Lachlan Orogen. Other findings include a large E–W-oriented region of elevated velocity beneath northern Victoria in the uppermost mantle that may be related to basaltic underplating associated with the formation of the Bass Basin during initial rifting of Australia and Antarctica (Rawlinson *et al.* 2011); elevated velocities beneath the Omeo Zone that point to the possibility that the Central Subprovince of the Lachlan Orogen is underlain by a large Proterozoic continental fragment of Rodinian origin (Rawlinson *et al.* 2011); and that the transition from lithosphere of Proterozoic continental origin to Phanerozoic oceanic origin occurs some 50 km east of the Tamar River in Tasmania (Rawlinson *et al.* 2010a).

One of the principal drawbacks of teleseismic tomography is that relative arrival time residuals are used instead of absolute arrival time residuals; this is necessary because of origin time uncertainty (which

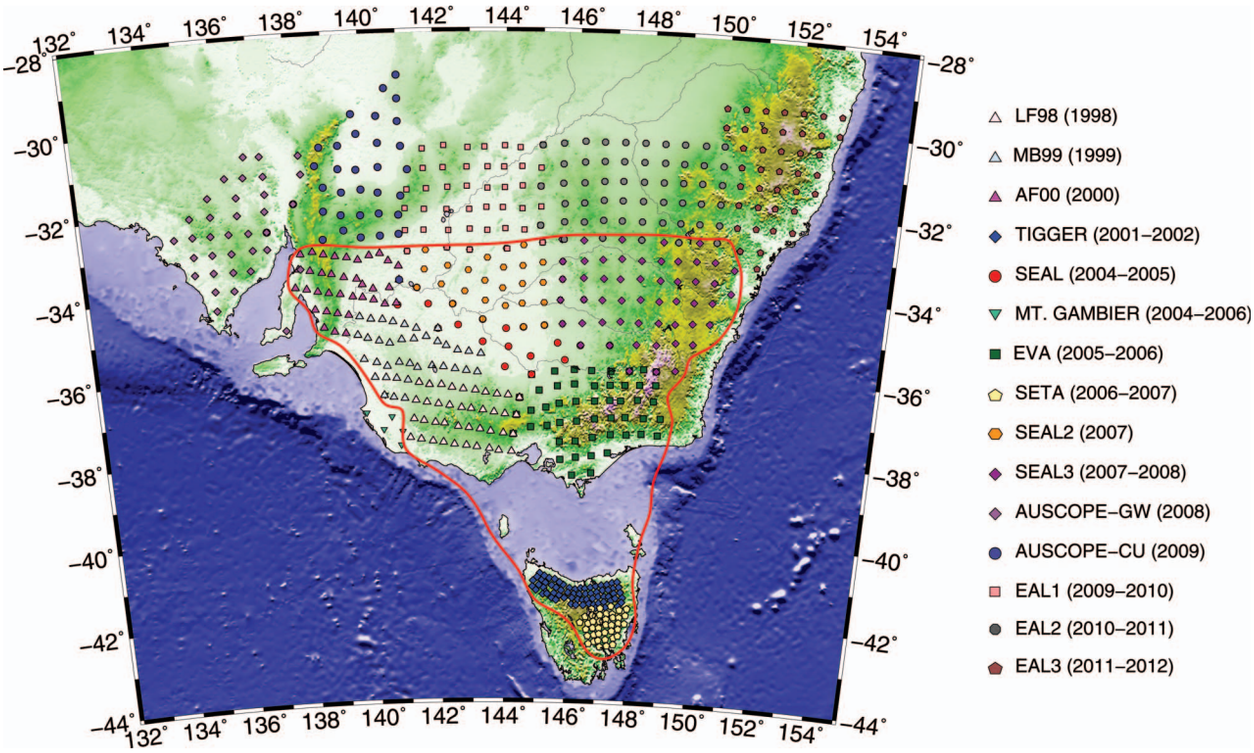

Figure 3 Map showing location of all WOMBAT stations in southeast Australia. All body wave data used in this study was recorded by the nine arrays that are enclosed by the thick red line.

can be much larger than the arrival time residuals) and variations in structure outside the 3-D model volume. As a consequence, lateral perturbations in wavespeed that are recovered are purely relative, and absolute wavespeed information is lost. This means that it becomes very difficult to compare models that are separately derived from data recorded by adjacent arrays. Joint inversion of multiple datasets for a single model mitigates this problem to some extent (Rawlinson *et al.* 2011), but long wavelength features (greater than the aperture of a single array) are lost. In a recent paper, Rawlinson & Fishwick (2011) use a starting model derived from surface wave tomography (Fishwick *et al.* 2008) in the inversion for P-wave velocity structure beneath southeast Australia. The long-wavelength features in the surface wave model in effect replace the information lost by using relative arrival time residuals. These new results provide a more complete picture of the lithosphere, and allow effects such as gradual lithospheric thinning towards the passive margins to be observed (Rawlinson & Fishwick 2011).

EVOLVING DATASETS

Methodology

SURFACE WAVE TOMOGRAPHY

A full description of the method used in the surface wave tomography is given in Fishwick *et al.* (2008), here we present a brief summary of the key components. In the present approach the construction of the shear wavespeed model for the whole continent can be considered in two parts. In the first stage a waveform inversion procedure (Cara & Leveque 1987; Debayle 1999) is used to calculate a 1D path-average velocity model (between source and receiver), which provides a good fit to an individual surface waveform. Given the non-linear dependence between the model parameters and the data, it is important to provide a reliable starting model for the inversion procedure. Within the crust, lateral heterogeneity is incorporated by using the global model 3SMAC (Nataf & Ricard 1996), and the crustal model remains fixed throughout the inversion process. For the mantle, we use multiple starting models. We first construct a preliminary model, using the data available from the work of Fishwick *et al.* (2008) that constrains the long-wavelength (>1000 km) variations in velocity throughout the study region. A reference path-average velocity can then be computed through this preliminary model; four different starting models are chosen that vary between $\pm 3\%$ from this reference. The results from each starting model are visually compared, and if all four models show similar characteristics, a final path-specific 1D model is calculated as a weighted average of each of these four models.

The second stage is the construction of the tomographic model. In this process, the information from all of the accepted path-specific 1D models is combined to determine the lateral variations in shear wavespeed. A series of depth slices are independently calculated at 25 km depth intervals; each 2D model is the result of a tomographic inversion relating the velocity

perturbation at a particular point to the set of path-specific information at this depth. Variations in velocity are parameterised using spherical B-splines, and the tomographic problem is solved using a damped least-squares inversion (see Fishwick *et al.* 2008 for full details). Strongly damped models are forced to remain close to an a priori reference model, whereas when no damping is applied the inversion will simply minimise the data misfit. Given the use of model norm damping, an appropriate a priori reference model is needed. One of the problems of using a radially averaged global reference model is that in the upper mantle, strong velocity contrasts exist between regions beneath the oceans and old continents, and forcing the final model back towards this mean velocity may not be meaningful. We continue to use the approach of Fishwick *et al.* (2005), where the tomographic inversion is carried out in two steps. The long-wavelength features required by the data are first recovered, and then a second tomographic inversion to obtain finer scale variations is performed that involves damping back towards this new, laterally heterogeneous reference model.

The dataset used in the present study consists of over 13 000 path-averaged models (compared with around 2600 in the previous studies). Given a fivefold increase in data it is not surprising that path coverage is significantly higher across the whole continent (see Figure 2b). Although the earlier ANU Research School of Earth Science temporary experiments (see Kennett 2003) had deployed many instruments within Western Australia, there remained relatively little data on the western margin of the continent. The inclusion of data from permanent stations, which are part of the Geoscience Australia network, has significantly increased path density in this region. Outside the continent, coverage is noticeably higher to the north-northwest and south-southeast (Figure 2). Additionally, the stations on islands to the east of Australia should improve reliability of the model within the Tasman Sea region. The eastern Indian Ocean remains the location with the lowest path coverage, and, for a regional scale study, this is unlikely to change without the deployment of ocean bottom seismometers.

BODY WAVE TOMOGRAPHY

The body wave tomography method used is described in Rawlinson *et al.* (2006a) and Rawlinson & Fishwick (2011), so only a brief summary is provided here. Model structure is represented using a regular grid of velocity points in latitude, longitude and depth, with an average spacing of $\sim$20 km. Cubic B-splines are then applied in order to define a smooth continuous medium. An iterative non-linear inversion method is used to adjust the velocity grid values in an attempt to satisfy the observations, subject to damping and smoothing regularisation. The initial model used for this study comes from the latest surface wave model described in this paper, which features much higher path density in southeast Australia compared with previous studies (see Figure 2).

Several assumptions have been made in order to combine the surface and body wave information. The surface wave model is described by absolute S-wave velocity variations, whereas the body wave dataset contains only P-wave arrival time residuals. The use of short period sensors means that higher frequency body waves from distant earthquakes are far more prevalent than lower frequency S-waves, so it is not possible to use the sparse S-wave dataset. As described previously, continent-wide P-wave velocity models are available, and in theory could provide an initial model for the inversion, but regional body wave coverage in southeast Australia is much poorer than surface wave coverage, which is why we favour using the S-wave model. In order to derive a P-wave model from the S-wave model, we simply assume ak135 Vp/Vs ratios owing to a lack of more detailed information. While this is an important assumption, which needs to be acknowledged, we note that in regions of similar spatial resolution in eastern Australia, the broad scale body and surface wave velocity models are in general agreement, so the likelihood of major artefacts being introduced is low.

The dataset used in the inversion comprises 25,834 arrival time residuals from 713 distant earthquakes that were cumulatively recorded by nine separate arrays—seven on the mainland and two in Tasmania (see Figure 3). Most arrival times are associated with direct P-waves, but PcP (reflections from the core–mantle boundary), PKiKP (reflections from the inner core boundary), PP (P-waves that reflect once from the surface of the Earth) and other global phases are also used. Relative arrival times are rapidly and accurately picked using the adaptive stacking method of Rawlinson & Kennett (2004), which exploits the coherency of waveforms detected at an array from a distant earthquake. Compared with the previous generation of combined body and surface wave results in southeast Australia published in Rawlinson & Fishwick (2011), the current study differs by including data from the two Tasmanian arrays, and using a significantly higher resolution surface wave model of the region.

RESOLUTION

Surface wave tomography

In order to illustrate the potential recovery of velocity structure given the path coverage used in the current study we present the results from a checkerboard reconstruction test with a 3-degree separation between minimum and maximum anomalies (Figure 4a). For each source–receiver path used in the real inversion, the average velocity is calculated through the synthetic checkerboard model. Gaussian noise is added to represent the uncertainties in the waveform inversion procedure, and the resulting dataset is inverted using the same procedure as for the real data. Throughout the continent the checkerboard structure is well recovered (see Figure 4b). The amplitudes of the recovered anomalies are slightly underestimated, which can be expected given the noise in the data and the regularisation scheme used within the inversion procedure. On the northwest margin of the continent, despite the improved path coverage (see Figure 2b) there remains

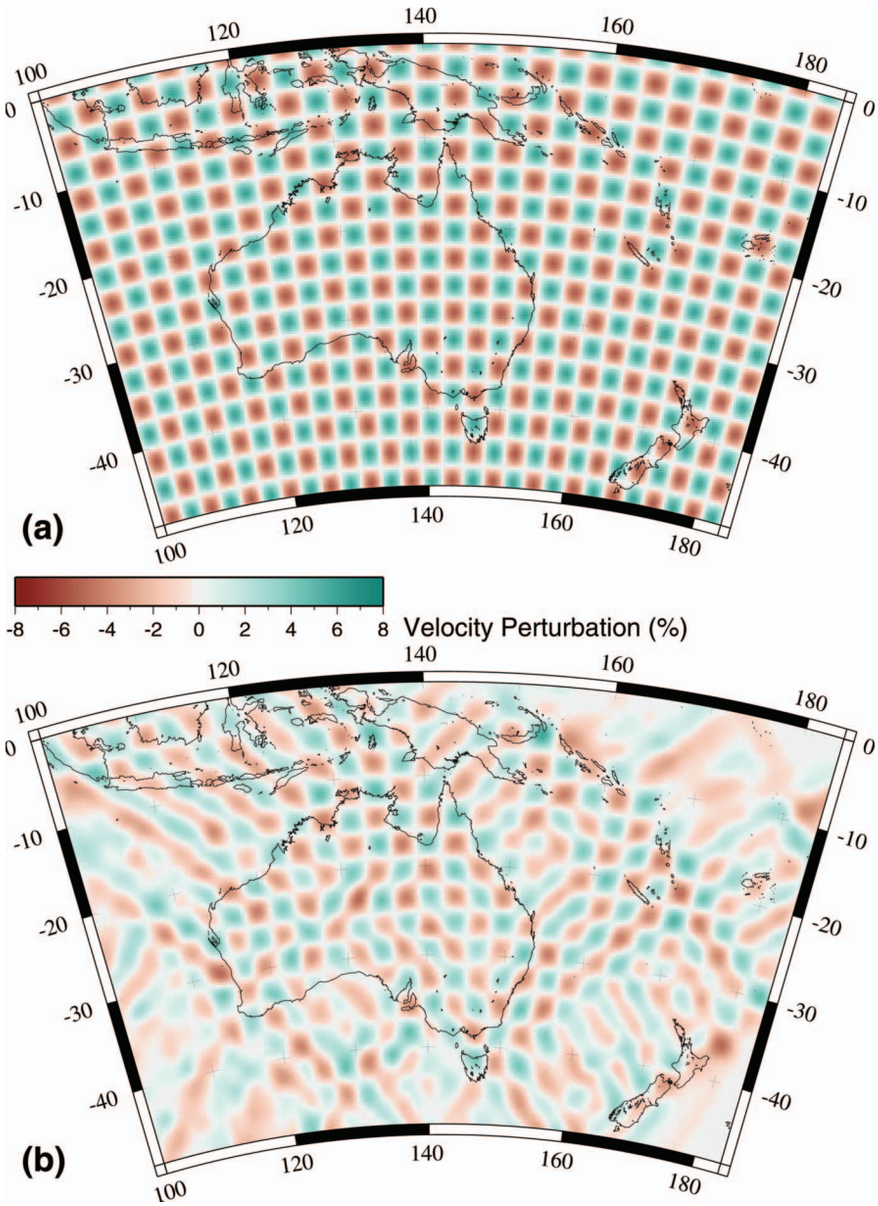

Figure 4 Checkerboard resolution test results for the surface wave dataset at a nominal depth of 100 km. (a) Illustration of the input model; (b) recovered velocity structure using the same path coverage as for the present study.

a tendency for anomalies to be smeared in a northwest–southeast direction; the dominant azimuth of path coverage in that region. To the west and south of the continent, despite the improved path coverage, structures with spatial scales in the order of 300 km can be difficult to resolve.

The result of the checkerboard test simply indicates the potential to recover structure for a particular depth slice. Given the two-stage nature of the surface wave tomography (see methodology) it is not possible to estimate the exact interdependence between the different layers (see also Simons *et al.* 2002). The vertical resolution of each 1D model is variable, as it is dependent on the data, the periods used, and whether higher mode information can be included in the waveform inversion. At this stage a full three dimensional estimate of resolution is therefore not feasible. However, previous surface wave studies have suggested that where higher mode information can be included, the vertical resolution will be in the order of 25–50 km in the uppermost mantle (Priestley *et al.* 2008).

Body wave tomography

As with the surface wave resolution tests above, we use a checkerboard reconstruction test to analyse the ability of the WOMBAT dataset to recover structure. Important differences to the above tests include: (1) only short scale length structure is recovered here; structures larger than the aperture of each array are only constrained by the surface wave dataset, so refer to the surface wave checkerboard test results when interpreting these features; (2) the checkerboard varies in latitude, longitude and depth, owing to the fact that 3-D structure is recovered in a single inversion. In order to simulate picking uncertainties associated with the observational dataset, Gaussian noise with a standard deviation of 50 ms is added to the synthetic arrival time residuals.

Figure 5 shows horizontal sections through the input and output checkerboard test model. The broad-scale variations in velocity structure are due to the presence of the laterally varying initial model. In general, the checkerboard pattern is well recovered beneath the region spanned by the arrays used in this study. Owing to the fact that body wave energy from distant earthquakes probes deep into the Earth before returning to the surface at a steep angle of incidence, there is little data coverage beneath the oceans (Figure 5, 100 km depth slice); that said, the gradual horizontal spread of the recovered checkerboard with increasing depth (cf. 100 km and 260 km depth slice in Figure 5) reflects the sub-vertical nature of the incoming rays.

Compared with the mainland, the quality of the checkerboard recovery beneath Tasmania is not noticeably superior, despite the fact that data density is much higher (owing to the smaller interstation spacing). Moreover, below 100 km depth, the recovered pattern becomes even less distinct. The reasons for these observations include the use of uniform regularisation throughout the model, the addition of data noise, and the fact that the aperture of the two Tasmanian arrays is much smaller than their mainland counterparts. In general, it can be shown for teleseismic tomography studies that the maximum depth of good resolution is approximately equal to two-thirds the aperture of an array (Evans & Achauer 1993); in the case of TIGGER this is around 170 km and in the case of SETA it is approximately 100 km. Thus, the accuracy of the checkerboard recovery at 180 km and 260 km depth (see Figure 5) is somewhat less than at 100 km depth beneath these two arrays.

One obvious feature of the recovered checkerboard anomalies is that amplitudes are universally underestimated; this is a recognised feature of gradient-based inversion methods that use damping and smoothing in an attempt to filter out structures that are not strongly constrained by the data (see Rawlinson *et al.* 2010b for more details).

EVOLVING MODELS AND TECTONIC IMPLICATIONS

Results

SURFACE WAVE TOMOGRAPHY

Figure 6 shows the results of the surface wave tomography at four different depths (75 km, 150 km, 225 km and 300 km). The results from the previous study of Fishwick *et al.* (2008) are included to illustrate the changes that have occurred owing to the increased data coverage and more detailed parameterisation. The variance reduction in the present study is – 75 km: 88.1%; 150 km: 91.1%; 225 km: 65.9%; 300 km: 21.1%. The very low variance reduction for the inversion at 300 km depth is due to two factors; first, the resolution of the surface wave tomography decreases with depth and there is likely to be a greater uncertainty in the path average velocity, and second, there are smaller velocity perturbations in the initial data, and as such a homogeneous starting model already provides a better fit to the data than the equivalent starting model at shallower depths. In comparison with the previous study there is a

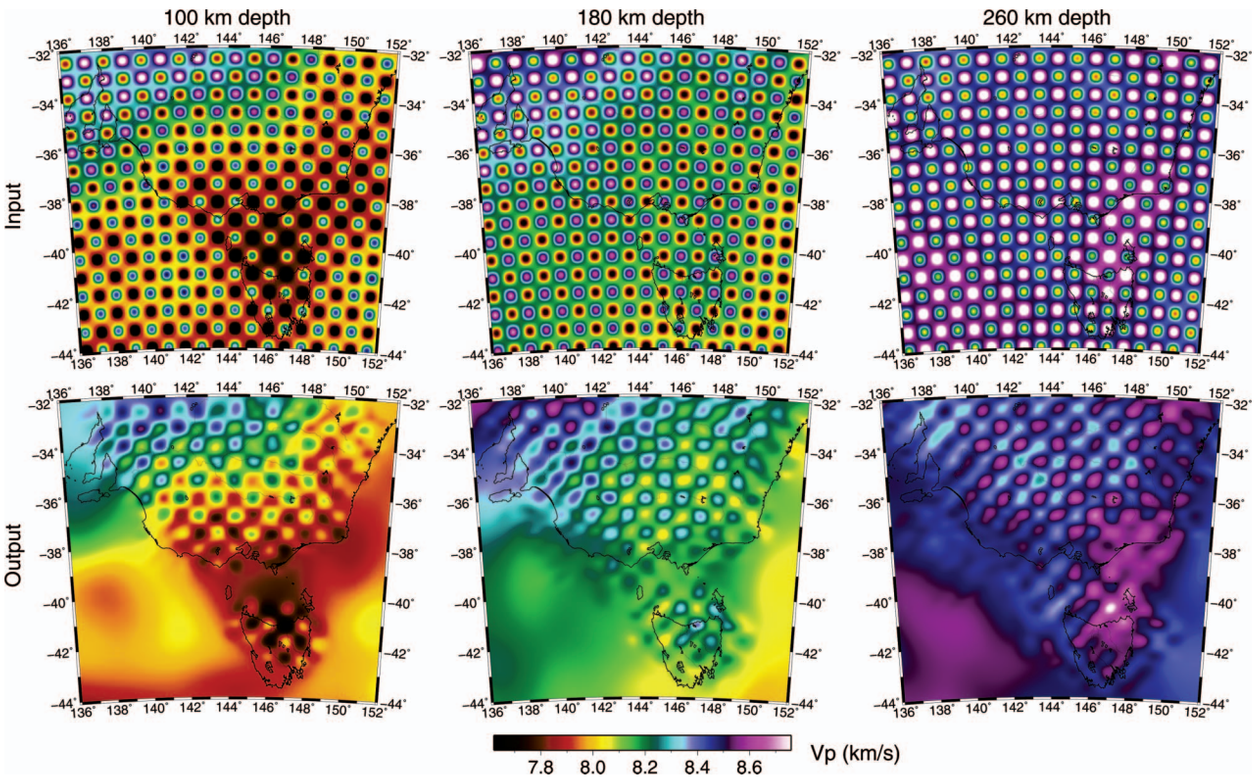

Figure 5 Checkerboard resolution test results for the body wave dataset at three different depths.

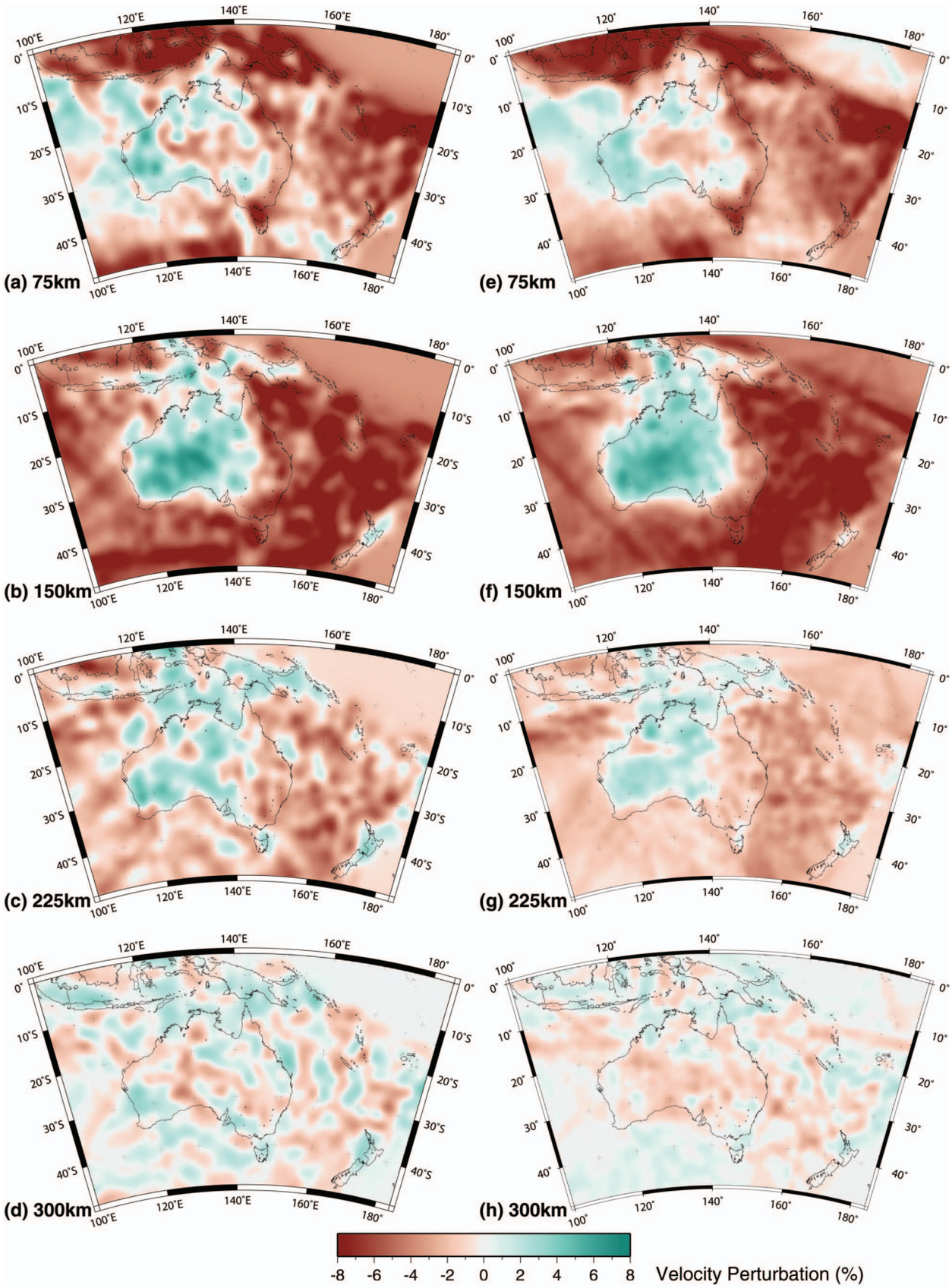

Figure 6 Surface wave inversion results at four different depths (75 km, 150 km, 225 km and 300 km). The left column (a–d) shows the results from the previous study of Fishwick *et al.* (2008), and the right column (e–h) shows the present results. Velocities are plotted as perturbations from the ak135 reference model, and the colour scale remains the same at all depths.

significant improvement in data fit in all but the deepest depth, for comparison the variance reduction in the earlier work was 82.5% at 75 km depth and 84.6% at 150 km depth (Fishwick *et al.* 2008). Again, there are likely to be two main reasons; first, the new data are predominately from permanent stations, which are inherently less noisy than temporary deployments of seismometers and should provide data with lower uncertainties, and second, the change in the parameterisation to a spline spacing with knot points at 1.5 degree intervals allows more variation in structure, which should enable a better fit to the data.

A visual comparison of the models (Figure 5) indicates that the broad scale features have changed very little. At the shallowest depths the slow velocities in central continue to be a distinct feature of the tomographic models. These low velocities are only observed in the uppermost mantle, and are underlain by faster seismic velocities at depths of 150 and 225 km, which is difficult to explain from simple models of constant composition and cratonic geotherms (see Fishwick & Reading 2008, for discussion). At 150 and 225 km depth comparison of the previous models (Figure 6b–c) and the new models (Figure 6f–g) indicates similar large-scale features, although in the latest models the strength of the velocity anomalies are more muted. This indicates that there is a slightly stronger damping used in the latest inversions. As the variance reduction remains significantly higher than the previous study, there is a trade-off between the lateral resolution of the parameterisation and the amplitudes of the velocity anomalies when fitting the data. At 300 km depth we observe the most significant variations between the old and new models. The fast velocities in the southwest of the continent (Figure 6d) are significantly reduced (Figure 6h); the extent to which this is the higher damping or the increased data in that region is difficult to determine.

BODY WAVE TOMOGRAPHY

Figures 7 and 8 show the results—as a series of horizontal depth slices—of the teleseismic body wave tomography that uses an initial model derived from surface wave tomography. Results from the previous

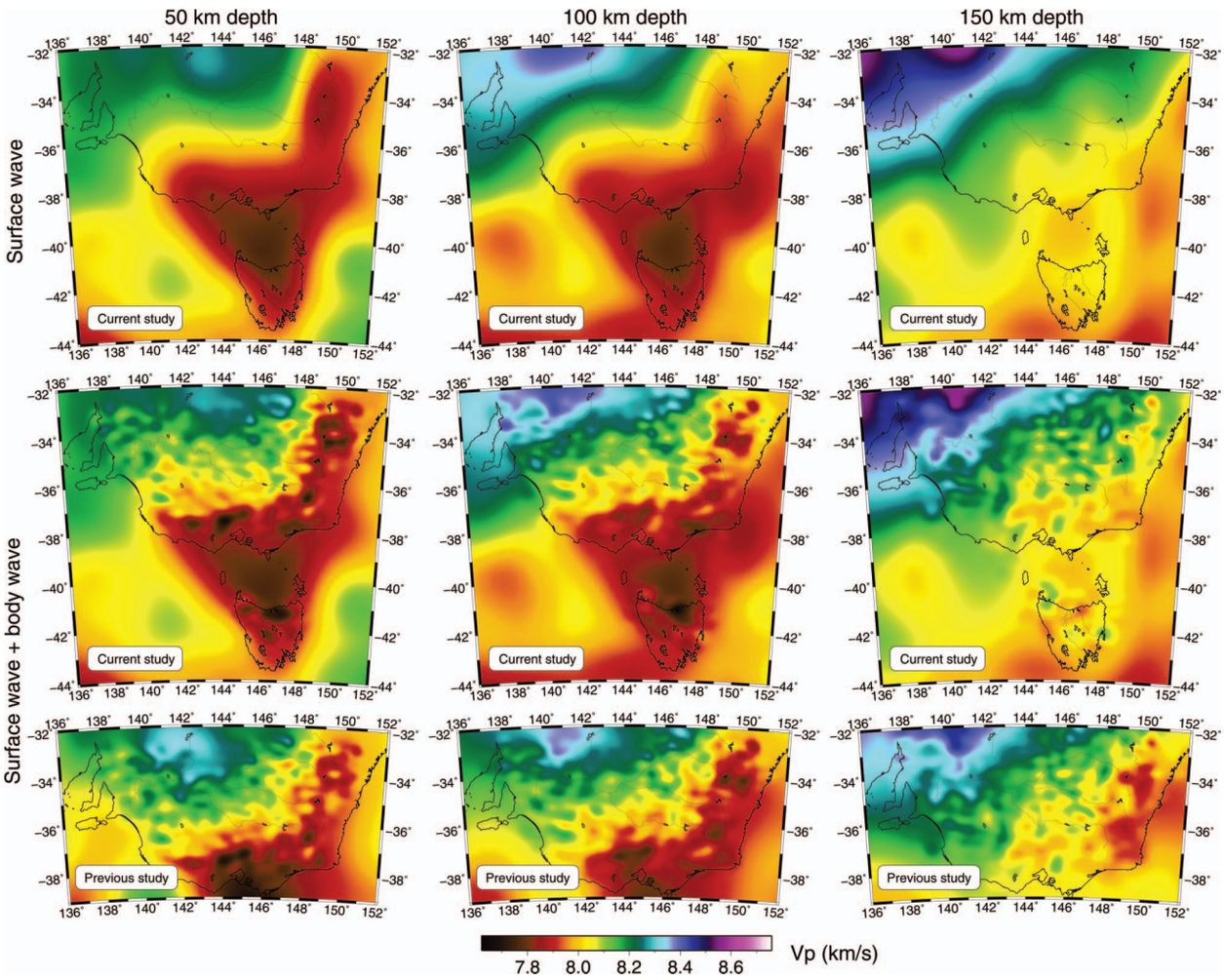

Figure 7 Body wave inversion results at three different depths (50 km, 100 km and 150 km). The top row shows the broad-scale structure of the surface wave only model; the middle row shows the combined body and surface wave results; and the bottom row presents the model from the previous study of Rawlinson & Fishwick (2011) for comparison. Note that in the latter case, the two Tasmanian datasets were omitted, which is why the plots do not extend further south than 39°.

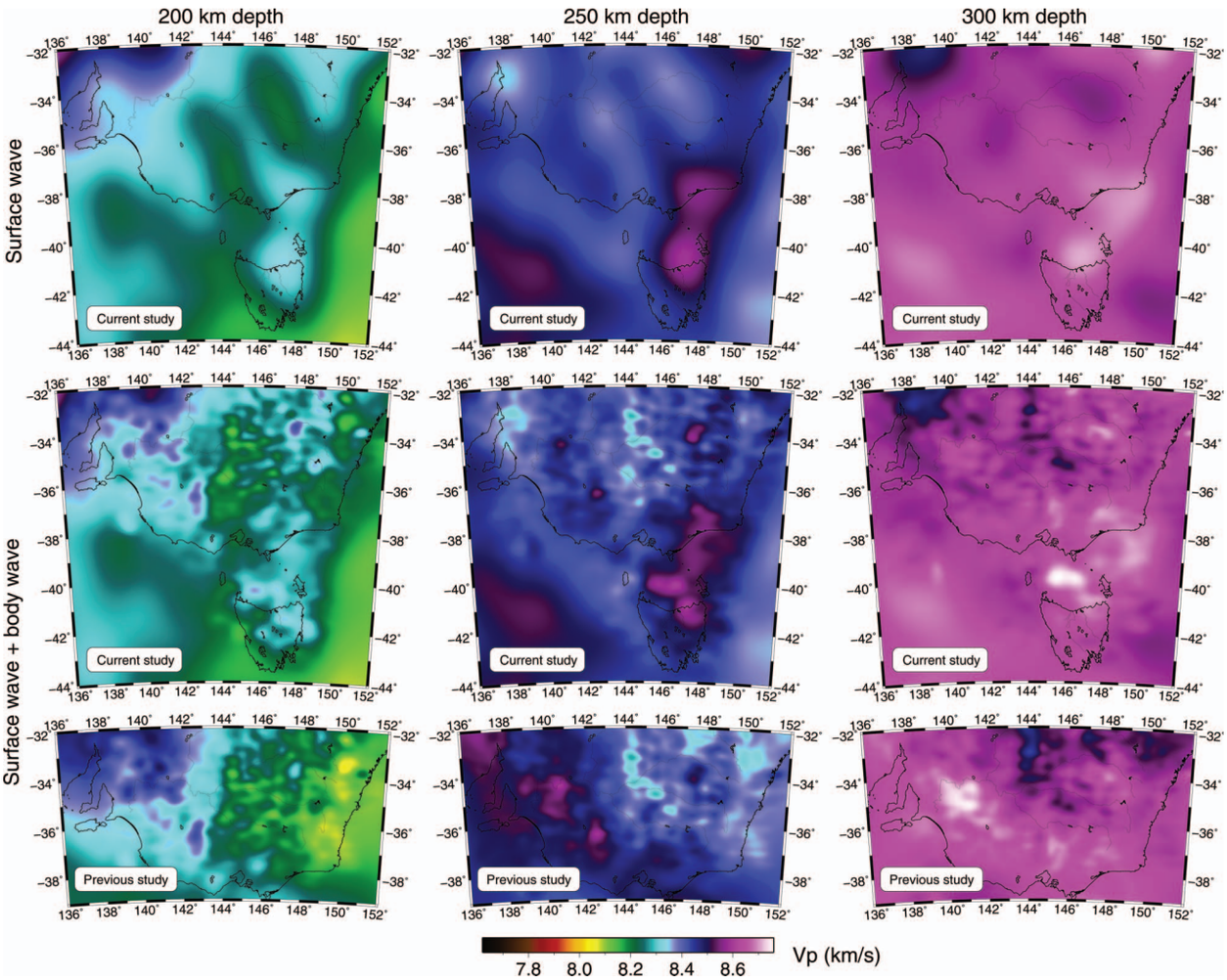

Figure 8 Same as Figure 6, but the three horizontal slices are taken at greater depths (200 km, 250 km and 300 km).

study of Rawlinson & Fishwick (2011), which use the surface wave model of Fishwick *et al.* (2008) and no data from Tasmania, are also included for comparison. Six iterations of the inversion scheme are used to achieve a 68% variance reduction in the data fit from 245 ms to 138 ms; additional iterations did not significantly improve the fit or change the visual appearance of the solution model. The remaining misfit can be attributed to data noise, limitations on permissible variations in structure imposed by the parameterisation and regularisation, and the underlying theory, which assumes that geometric ray theory is valid. The introduction of teleseismic body wave constraint via traveltime inversion clearly introduces short wavelength features, while generally preserving the long-wavelength features present in the initial model. It is important to view these results in light of the checkerboard resolution tests (Figure 5), which clearly show that the body waves offer little constraint outboard of Tasmania and the mainland, which is why the solution models tend to revert to the starting model in areas submerged by oceans. Furthermore, it is necessary to consider the resolution of the surface wave models (see Figure 4) when interpreting the final model, because the long-wavelength features are not uniformly constrained; for example, the triangular low-velocity zone between 50 and 100 km depth beneath northern Tasmania and Bass Strait may partly be a function of crossing path distribution.

The differences between the current results and those of Rawlinson & Fishwick (2011) can be observed largely in the longer wavelength structures, although some variations in shorter wavelength features can be detected owing to the use of slightly different regularisation. The main difference between the models occurs near the east mainland coast at 200 km depth, where the velocities in the current study are significantly higher than the previous study. This attribute is largely inherited from the updated surface wave model.

West Australian Cratons

The geological structure of western Australia is dominated by the Yilgarn and Pilbara cratons (see Figure 1). These two Archean cratons form the majority of the West Australian Craton, and contain much of the oldest preserved crustal material in the Australian continent. The Capricorn Orogen records a series of Paleoproter-

ozoic events related to the joining of the Pilbara and Yilgarn cratons, and had subsequent reactivation through into the Neoproterozoic (see Cawood & Korsch 2008). The West Australian Craton is bounded by a number of Proterozoic orogens: the Albany-Fraser Orogen to the southeast, the Paterson Orogen to the northeast and Pinjarra Orogen to the west. The other cratonic region that is discussed with respect to the surface wave results is the Kimberley Block. Part of the North Australian Craton, the majority of the Kimberley is overlain by ancient sediments and little of the original basement is exposed. Isotopic data from diamondiferous kimberlites suggest that the Archean lithospheric mantle existed beneath the Kimberley Block (Graham *et al.* 1999; Downes *et al.* 2007). The highest concentration of diamondiferous intrusions in Australia is found on and at the margins of the Kimberley Block (Jaques & Milligan 2004).

Figure 9 illustrates the absolute shear velocities from the surface wave tomography throughout western Australia at depths of 100 and 200 km. At the shallowest depth slice, the West Australian Craton is clearly stands out as a clear high velocity anomaly. Within this region, there are also noticeable differences in velocity structure between the Yilgarn and Pilbara Cratons, and the Capricorn Orogen. At 100 km depth velocities of $\sim$4.75 km/s are observed beneath both Archean cratonic regions, whereas slower velocities of $\sim$4.65 km/s are found beneath the Capricorn Orogen. Recent work, using seismic receiver functions, has also indicated a compatible variation in structure. Reading *et al.* (2012) find that beneath the orogen, the transitions at the Moho are much less distinct, mid-crustal character more complex, and mantle wavespeed is generally slower than at stations beneath the adjacent Cratons. The results of the present surface wave study suggest that this is a consistent feature beneath the Capricorn Orogen, and not just associated with local structure beneath a seismic station. The contrast in velocity of $\sim$0.1 km/s could be caused by a number of factors such as temperature, composition or grainsize. Compositional variations could relate to the initial mantle depletion or to mantle refertilisation through processes that occurred during reactivation (Reading *et al.* 2012). Unravelling the combination of different components of the velocity anomaly is not possible from the tomographic study alone.

At 200 km depth, the Pilbara and Yilgarn Cratons no longer have the same seismic velocity structure (Figure 9). Beneath the Pilbara, a relatively low-velocity zone ($\sim$4.55 km/s in comparison with 4.75 km/s at depths around 100 km) is observed. This decrease in velocity is expected through the continental lithosphere as the effects of increasing temperature have a stronger influence on velocity than the increasing pressure. Beneath much of the Yilgarn, almost no low-velocity zone is observed. The Kimberley Block is particularly evident as a fast velocity anomaly at 200 km depth, although somewhat to the south of the surface expression. Given the proximity of the diamondiferous kimberlites (Jaques & Milligan 2004), it would be expected to see fast velocity anomalies representative of a region of thicker lithosphere. Whether the slow velocities (4.47–4.6 km/s) at 100 km are indicative of compositional layering within the lithosphere is uncertain, but they are not easily explained by simple cratonic geotherms and constant composition (see e.g. Faul & Jackson 2005).

Figure 9a includes additional information on the location of gold deposits (historic mines and mineral deposits) found in Western Australia. Given the interest in using geophysical observations to help understand, and predict, potential locations of mineralisation (e.g. Blewett *et al.* 2010; Czarnota *et al.* 2010) it is worth considering these broad-scale observations. The majority of the deposits appear to be found close to the edge of the high velocity foci within Western Australia; this relationship is visible for deposits adjacent to both the Pilbara and Yilgarn Craton. In contrast to the earlier work looking specifically at the Eastern Goldfields (Blewett *et al.* 2010; Czarnota *et al.* 2010), we do not advocate using a particular velocity contour as a predictive tool; it certainly would not be applicable from one regional inversion to another. As the comparison of the tomographic models shows (Figure 6), the absolute velocities that are recovered are strongly dependent on the parameterisation and regularisation used within the inversion scheme. However, the visual correlation of the location of the mineral deposits with the margins of the fastest velocities, strongly suggests that a more detailed comparison of mantle structure with respect to mineralisation would be very valuable in this region.

Tasman Line

Although the concept of the Tasman Line remains linked to the transition from the Precambrian Shield of central Australia to the Phanerozoic terranes in the east, Direen & Crawford (2003) illustrated that the geophysical anomalies that have been interpreted as a single line have no clear relation to a Rodinian-rifted margin. Instead the geophysical anomalies document a protracted geological history, recording events from the Neoproterozoic through to the Carboniferous (Direen & Crawford 2003). The unravelling of any mantle seismic signature, associated with the transition has been discussed by Kennett *et al.* (2004b) and Fishwick *et al.* (2008) and we use the latest results to describe how the evolving dataset provides further information on the deep structure. Figure 10 illustrates the horizontal gradient in seismic velocity for a series of slices through the surface wave model. Plotting the horizontal gradient emphasises regions of strong lateral variations, and has the distinct advantage over the tomographic model itself; in that the results are independent to the choice of reference model and colour scheme (see Fishwick 2006, for further discussion). For comparison, the results from the present study have been overlain by four lines indicating the regions of strongest horizontal gradients in seismic velocity that were observed in the earlier tomographic study of Fishwick *et al.* (2008).

In concurrence with the earlier results, the strongest continuous velocity gradient is clearly observed on the eastern margin of the continent, inland of the continent–ocean transition. The significant increase in data, and more detailed parameterisation, has made only minor

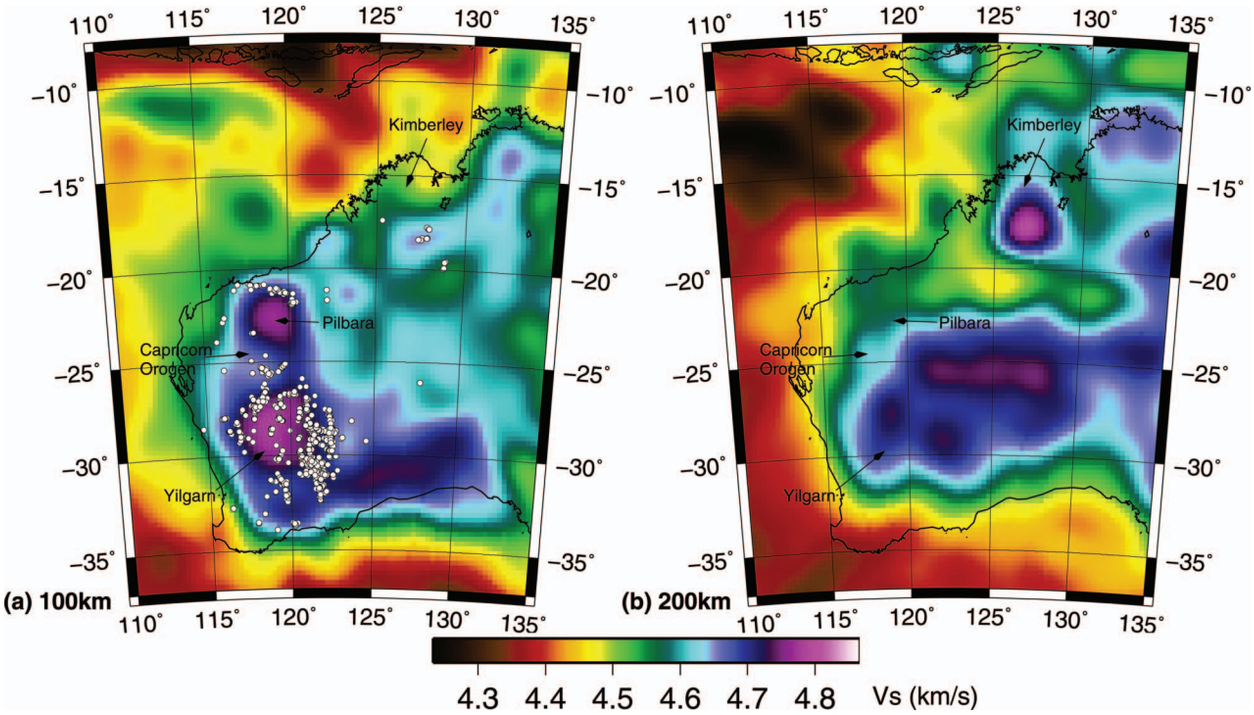

Figure 9 Absolute velocities determined from the surface wave inversion: (a) 100 km; white circles mark the location of all known gold deposits. Locations are taken from the Australian Atlas of mineral resources, mines and processing centres (<http://www.australianminesatlas.gov.au/>); (b) 200 km.

changes to the location of this change in velocity. In fact, at the shallowest depth (75 km) the strongest gradients in northern Victoria and southern New South Wales (32–35°S) occur in an almost identical position in the new tomography models (Figure 9a). The updated tomography and fixed location of the velocity gradients provide strong evidence that the link between the Cenozoic volcanism on the eastern margin of Australia and the lithospheric structure (see Fishwick *et al.* 2008) is a robust one. The results at 125 km depth suggest that this transition in lithospheric structure is not vertical but in fact dips towards the west (Figure 10b). The stronger velocity gradient follows a similar pattern but is shifted by approximately 200 km further inland.

This westerly dip in structure is a distinct change to the previous models, where a slight eastward dip had been inferred from the velocity model.

The westernmost transition is associated with the edge of the thick lithosphere beneath Mt Isa, central Australia and the Curnamona province. In the study by Kennett *et al.* (2004a) the transition from fast to slow velocities was found to be in an approximately north–south line close to 140°E. The addition of data from the TASMAL experiment created a distinct change in shape to the transition, with the strong gradients observed further to the west in central Australia (Fishwick *et al.* 2008). In the latest models, the magnitude of the velocity gradient is smaller; however, the location has remained in approximately the same position. Given the different regularisation used in the two inversions (see Results), it is not surprising that the absolute values of the horizontal gradient also change. While the present study has incorporated data from very few new seismic stations in the vicinity of this transition, the overall path coverage has significantly increased (see Figure 2). The stability of the large-scale structure between the recent models is encouraging and suggests that in order to gain a more detailed picture of the transition, new stations would be required.

Fishwick *et al.* (2008) also inferred a central transition (marked by the dashed-dot line) on the basis of the velocity gradients, changes in anisotropic structure, and the absolute velocities within each region. In the new models presented in Figure 10, this transition is clearly less coherent. There are localised velocity gradients, which trend from NNW–SSE to NNE–SSW, observed at the various depths, but there is no evidence of a single coherent transition. Based on geochemical evidence in the south of the continent (e.g. Handler & Bennett 2001), this transition had been related to the margin of Proterozoic lithospheric mantle. However, further north, the lack of outcrop or geochemical information beneath the Thomson Orogen provides no additional constraints. The latest surface wave model suggests that this transition is more complex than previously imaged. Given the variations in velocity observed from the local body wave studies, this is perhaps not surprising, and the combined results (see following section) should elucidate the detailed structure of this region.

South East Australia

The southeast portion of the Australian plate comprises the Phanerozoic Lachlan and Delamerian Orogens, the latter commonly referred to as the Tyennan Orogen in

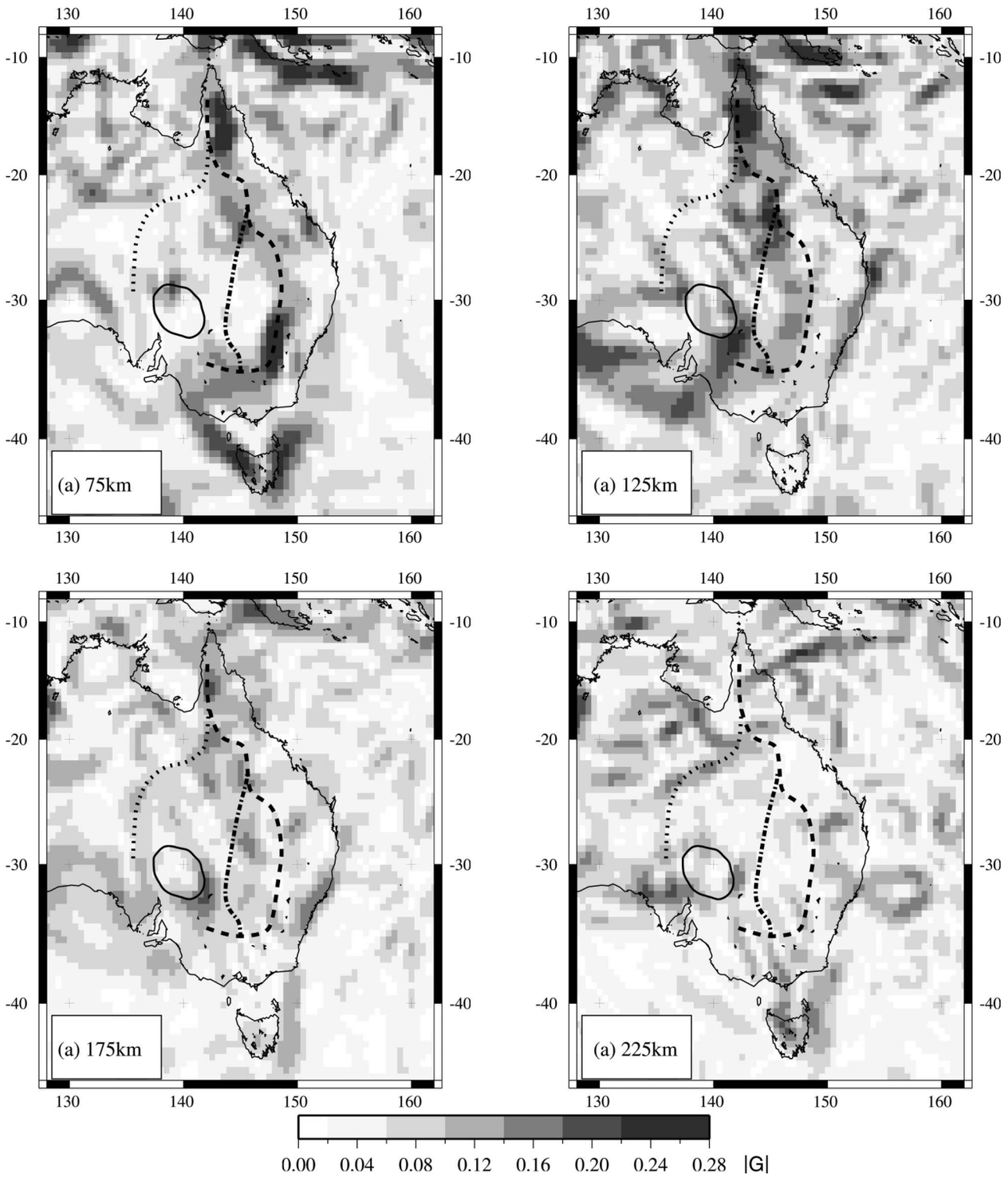

Figure 10 Maps showing the magnitude of the horizontal gradient, G, as calculated using the approach of Fishwick (2006). Lines indicate distinct regions of strong gradient as defined from the earlier surface wave study: solid line indicates region of fast velocities associated with the Curnamona Block; dashed line indicates strong gradients at shallow mantle depths (75–150 km); dot-dash line indicates gradients that were observed at 150–200 km depth; dotted line indicates gradients that were observed at 200–250 km depth and associated with the margin of the Precambrian shield (Fishwick *et al.* 2008).

Tasmania (e.g. Crawford *et al.* 2003). These orogens formed outboard of the East Gondwana margin largely through a process of subduction accretion, and are thought to contain lithosphere of oceanic origin, and reworked Precambrian continental lithosphere (see Betts *et al.* 2002 and Glen 2005 for comprehensive reviews and discussions). Subsequent to their formation, events such as the separation of Australia and Antarctica and the opening of the Tasman Sea at between 90–80 Ma, the formation of late Mesozoic and

Cenozoic basins (e.g. the Murray Basin), and the advent of Cenozoic volcanism inboard of the east coast of Australia, have conspired to make the task of unravelling the Paleozoic evolution of the continent very difficult (see Rawlinson & Fishwick 2011 for more details). The latest results seek to provide new information on the structure of the Paleozoic orogens at upper mantle depths and examine whether there is any correlation between features in the lithospheric mantle and surface expressions of both recent volcanism and zones of mineralisation.

Figure 11 shows a selection of depth sections from the body wave tomography with inferred boundaries and several types of data superimposed. Figure 11a superimposes topography, bathymetry and the locations of Cenozoic volcanic remnants. Inboard of the east coast, the N–S-trending zone of low velocity conforms quite accurately with the elevated topography of the southern Great Dividing Range. Owing to the vertical smearing inherent in body wave tomography, some aspect of the observed lower velocities is likely to be due to the deep crustal root, needed for isostatic support, beneath the mountain range. Another contributor is likely to be lithospheric thinning in the neighbourhood of the passive margin associated with the break-up of Australia and Antarctica and the opening of the Tasman Sea.

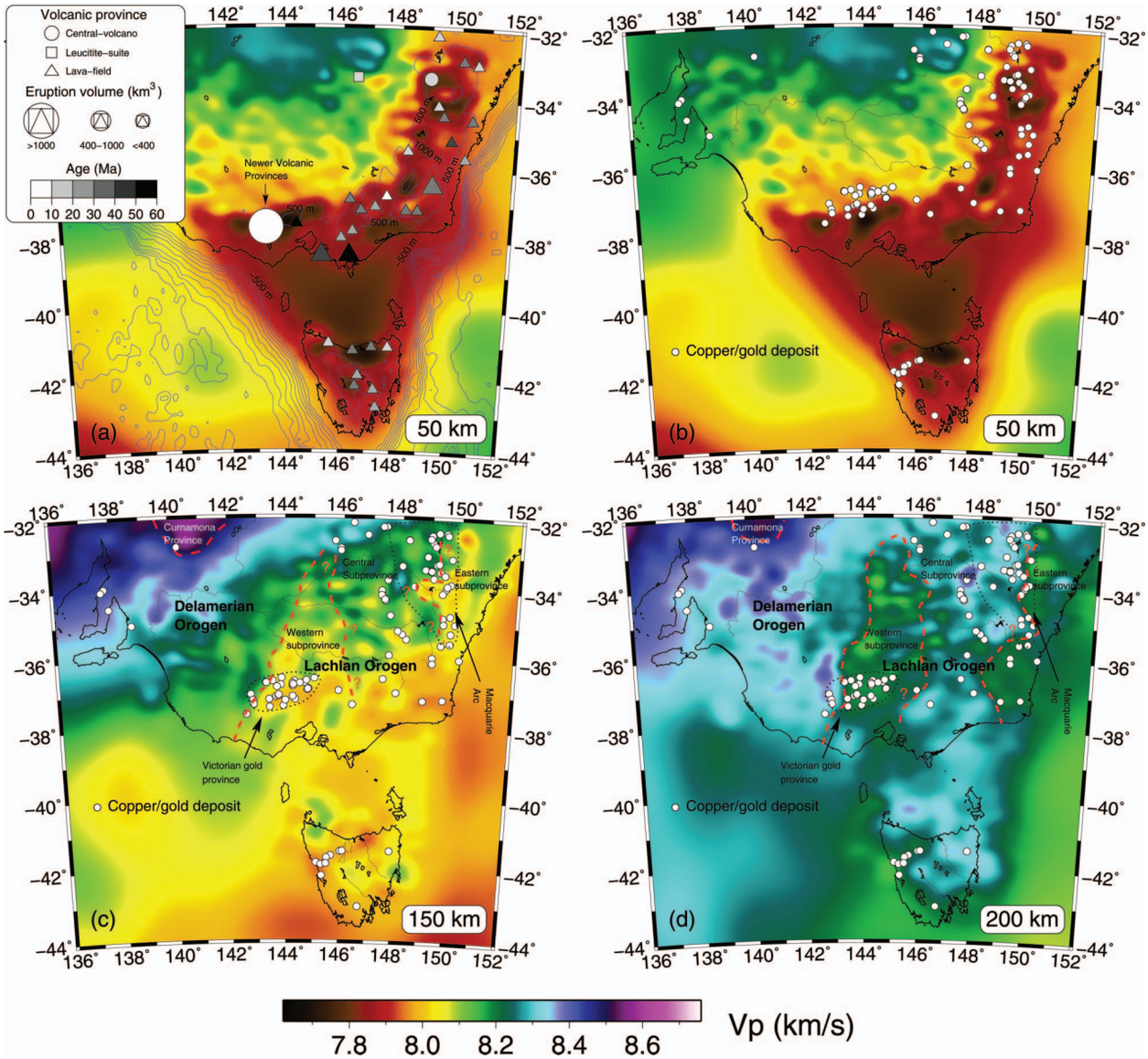

Figure 11 Depth slices with data and inferred boundaries superimposed. (a) 50 km depth slice with topography, bathymetry and Cenozoic volcanic zones superimposed. Topography and bathymetry data are sourced from the Etopo2 global dataset, and is contoured every 500 m. The volcanic province database is taken from Johnson (1989). (b) 50 km depth slice with the location of all known copper/gold deposits superimposed. Locations are taken from the Australian Atlas of mineral resources, mines & processing centres (<http://www.australianminesatlas.gov.au/>). (c) 150 km depth slice with copper–gold deposits and inferred province boundaries marked. (d) 200 km depth slice with copper/gold deposits and inferred province boundaries marked.

The fact that almost all volcanic centres and lava fields overlie low velocity regions is likely to be related to the presence of a thin lithosphere. In the case of the Quaternary Newer Volcanics province, which does not overlie significantly elevated topography, the lower velocities that can clearly be observed in the underlying mantle are most likely due to the elevated temperatures associated with a hot spot source. The fact that the lower velocity anomalies cannot be observed below 150 km depth could indicate that the hot spot is localised in the uppermost mantle. If so, the presence of a thermal anomaly of this magnitude may be explained by edge-driven convection (e.g. Demidjuk *et al.* 2007; Farrington *et al.* 2010). However, plumes have a propensity to broaden on contact with the lithosphere (e.g. Moore *et al.* 1998), so it is plausible that one is present, but cannot be detected at depth owing to the resolution limits of the body wave dataset.

Figure 11b shows the same depth slice as Figure 11a but instead superimposes the locations of known copper–gold deposits. The large region inboard of the coast in which copper/gold deposits are absent corresponds closely with the presence of the Murray Basin, which masks the basement rocks. Figure 11c, d shows slices at 150 km and 200 km depth with known copper–gold deposits and inferred boundaries superimposed. One of the main features of these images is a strong west–east transition from higher to lower velocities that we regard as a strong signature of the boundary between the Delamerian and Lachlan orogens in the upper mantle. The location of this boundary is consistent with an east-dipping Moyston Fault, which has been detected by seismic reflection profiling in the deep crust (Korsch *et al.* 2002). There are two possible reasons for the observed velocity contrast: (1) a velocity contrast between Proterozoic mantle lithosphere in the west and Paleozoic mantle lithosphere in the east; and (2) a velocity contrast between mantle lithosphere in the west and sublithospheric mantle in the east. We favour the latter explanation because the lithosphere beneath the Lachlan Orogen is unlikely to be much thicker than 100 km (Fishwick *et al.* 2008), whereas the adjoining Proterozoic lithosphere could be up to 200 km thick. Moreover, there is little evidence of a strong velocity contrast in this location at depths of 50 km and 100 km. However, the overprinting effects of the Newer Volcanics province, separation of Australia and Antarctica and opening of the Tasman Sea on the velocity field are difficult to decouple from other tectonic events. For instance, the elevated temperatures associated with the Newer Volcanics province may well obscure the presence of a lithospheric boundary in Victoria, and mafic underplating associated with the possible formation of asymmetric passive margins during rifting in the Cretaceous (e.g. Lister *et al.* 1986) may overprint Paleozoic velocity variations.

Based on geological and geochemical data collected at the surface, as well as potential field data, the Lachlan Orogen has been divided into several subprovinces (e.g. Foster & Gray 2000). Evidence for these subprovinces in the upper mantle is rather tenuous, with the red dashed lines superimposed in Figure 11c, d denoting possible boundaries. Other features of interest include a distinct velocity high beneath the paleo-Proterozoic Curnamona Province (Conor & Preiss 2008), which suggests that the lithosphere is thicker and faster in this region compared with the younger lithosphere to the southeast. The elevated velocities beneath eastern Victoria, Bass Strait and northern Tasmania (Figure 11d) provides some traction to the idea that Tasmania and Victoria are joined by a Proterozoic micro-continent that was embedded during the formation of the Tasmanides (Cayley *et al.* 2002), but if so, it is not clear why a positive velocity anomaly is not visible at shallower depths.

It is interesting to note that at depths of 150–200 km, the copper/gold deposits tend to occur near the edge of velocity transition zones (see Figure 11); for instance the Victoria gold province is located near the major inferred boundary between the Lachlan and Delamerian orogens, while deposits in the Macquarie Arc tend to be concentrated along the inferred boundary between the Central and Eastern subprovinces of the Lachlan Orogen. In a previous study, Rawlinson *et al.* (2011) suggested that a substantial fragment of Precambrian lithosphere—possibly paleocratonic—may underlie the Central Subprovince, which would explain the elevated velocities that are observed. These results appear to be consistent with the surface wave results discussed above, which show a correlation between the edge of a cratonic block in Western Australia and the distribution of known gold deposits.

CONCLUSIONS

Despite the fivefold increase in data for the surface wave model, the large-scale features remain very similar to the earlier tomography models. The most noticeable changes are in areas with additional 584 stations; for example, the inclusion of data from the Geoscience Australia network in Western Australia has altered the velocity structure in the Yilgarn Craton. The new models show slightly lower amplitude variations in velocity—the results of the finer parameterisation and different choices in damping. Therefore, the absolute velocities that are recovered in the surface wave tomography are very much dependent on the regularisation of the inversion. Although this does not significantly alter the interpretations of the large-scale features, care must be taken in assuming any direct relationship between particular velocities and geological features. The horizontal gradients in velocity continue to indicate a series of distinct changes in lithospheric structure in the east of the continent. In the present study, the central transition in Victoria–New South Wales is considerably more complex than in the previous lower-resolution models (Fishwick *et al.* 2008).

In Victoria, the region of this central transition is in the middle of the WOMBAT array, and the detailed body wave tomography indicates why any transition may be difficult to image at a more regional scale. The results (Figures 7, 10) clearly show significant small-scale variations in structure. A change in velocity that

correlates with the east-dipping Moyston fault is interpreted as the boundary between the Delamarian and Lachlan Orogen, and a region of faster velocities may demarcate the Central Subprovince of the Lachlan Orogen. These variations in structure at scales of 50–200 km will be very difficult to image with the present surface wave methodology. In the uppermost mantle, the latest body wave tomography does confirm very low velocities beneath the Newer Volcanics province and on the eastern margin of the continent.

ACKNOWLEDGEMENTS

We would like to thank all those involved in the establishment of permanent seismic stations and networks in the area. A large amount of fieldwork has been undertaken by the Research School of Earth Sciences, Australian National University; to all those who have been involved in this program, we offer great thanks. The facilities of the IRIS Data Management centre have been used to access much of the data. S. Fishwick's work has been funded by NERC New Investigator grant NE/G000859/1. N. Rawlinson's contribution is supported by ARC Discovery Proposal DP0986750.

REFERENCES

Begg G. C., Hronsky J. A. M., Arndt N. T., Griffin W. L., O'Reilly S. Y. & Hayward N. 2010. Lithospheric, cratonic, and geodynamic setting of Ni–Cu–PGE sulphide deposits. *Economic Geology* **105**, 1057–1070.

Betts P. G., Giles D., Lister G. S. & Frick L. R. 2002. Evolution of the Australian lithosphere. *Australian Journal of Earth Sciences* **41**, 661–695.

Blewett R. S., Henson P. A., Roy I. G., Champion D. C. & Cassidy K. F. 2010. Scale integrated architecture of a world-class gold mineral system: the Archaean Eastern Yilgarn Craton, Western Australia. *Precambrian Research* **183**, 230–250.

Boschi L. & Ekström G. 2002. New images of the Earth's upper mantle from measurements of surface wave phase velocity anomalies. *Journal of Geophysical Research* **107**, doi:10.1029/2000JB000059.

Cara M. & Leveque J. J. 1987. Waveform inversion using secondary observables. *Geophysical Research Letters* **14**, 1046–1049.

Cawood P. A. & Korsch R. J. 2008. Assembling Australia: Proterozoic building of a continent. *Precambrian Research* **166**, 1–38.

Cayley R., Taylor D. H., VandenBerg A. H. M. & Moore D. H. 2002. Proterozoic–Early Palaeozoic rocks and the Tyennan Orogeny in central Victoria: the Selwyn Block and its tectonic implications. *Australian Journal of Earth Sciences* **49**, 225–254.

Cleary J. 1967. P times to Australian stations from nuclear explosions. *Bulletin of the Seismological Society of America* **57**, 773–781.

Clifford P., Greenhalgh S., Houseman G. & Graeber F. 2008. 3-D seismic tomography of the Adelaide fold belt. *Geophysical Journal International* **172**, 167–186.

Conor C. H. H. & Preiss W. V. 2008. Understanding the 1720–1640 Ma Palaeoproterozoic Willyama Supergroup, Curnamona Province, Southeastern Australia: Implications for tectonics, basin evolution and ore genesis. *Precambrian Research* **166**, 297–317.

Crawford A. J., Cayley R. A., Taylor D. H., Morand V. J., Gray C. M., Kemp A. I. S., Wohlt K. E., VandenBerg A. H. M., Moore D. H., Maher S., Direen N. G., Edwards J., Donaghy A. G., Anderson J. A. & Black L. P. 2003. Neoproterozoic and Cambrian continental rifting, continent–arc collision and post-collisional magmatism. *In*: *Evolution of the Palaeozoic Basement*, pp. 73–93. Geological Society of Australia, Sydney, Australia.

Czarnota K., Blewett R. S. & Goscombe B. 2010. Predictive mineral discovery in the eastern Yilgarn Craton, Western Australia: An example of district scale targeting of an orogenic gold mineral system. *Precambrian Research* **183**, 356–377.

Debayle E. 1999. SV-wave azimuthal anisotropy in the Australian upper mantle: preliminary results from automated Rayleigh waveform inversion. *Geophysical Journal International* **137**, 747–754.

Debayle E. & Kennett B. L. N. 2000. The Australian continental upper mantle: structure and deformation inferred from surface waves. *Journal of Geophysical Research* **105**, 25423–25450.

Demidjuk Z., Turner S., Sandiford M., George R., Foden J. & Etheridge M. 2007. U-series isotope and geodynamic constraints on mantle melting processes beneath the Newer Volcanic Province in South Australia. *Earth and Planetary Science Letters* **261**, 517–533.

Direen N. G. & Crawford A. J. 2003. The Tasman line: where is it, what is it, and is it Australia's Rodinian breakup boundary? *Australian Journal of Earth Sciences* **50**, 491–502.

Downes P. J., Griffin B. J. & Griffin W. L. 2007. Mineral chemistry and zircon geochronology of xenocrysts and altered mantle and crustal xenoliths from the Aries micaceous kimberlite: constraints on the composition and age of the central Kimberley Craton Western Australia. *Lithos* **93**, 175–198.

Evans J. R. & Achauer U. 1993. Teleseismic tomography using the ACH method: theory and application to continental scale studies. *In*: Iyer H. M. & Hirahara K. eds. *Seismic tomography: theory and practice*, pp. 319–360. Chapman & Hall, London.

Farrington R. J., Stegman D. R., Moresi L. N., Sandiford M. & May D. A. 2010. Interactions of 3D mantle flow and continental lithosphere near passive margins. *Tectonophysics* **483**, 20–28.

Faul U. H. & Jackson I. 2005. Seismic signatures of temperature variations in the upper mantle. *Earth and Planetary Science Letters* **234**, 119–134.

Fichtner A., Fishwick S., Yoshizawa K. & Kennett B. L. N. 2012. Optimal spherical spline filters for the analysis and comparison of regional-scale tomographic models. *Physics of the Earth and Planetary Interiors* **190–191**, 44–50.

Fichtner A., Kennett B. L. N., Igel H. & Bunge H-P. 2009. Full seismic waveform tomography for upper mantle structure in the Australasian region using adjoint methods. *Geophysical Journal International* **179**, 1703–1725.

Fichtner A., Kennett B. L. N., Igel H. & Bunge H-P. 2010. Full waveform tomography for radially anisotropic structure: New insights into present and past states of the Australasian upper mantle. *Earth and Planetary Science Letters* **290**, 270–280.

Fishwick S. 2006. Gradient maps: A tool in the interpretation of tomographic images. *Physics of the Earth and Planetary Interiors* **156**, 152–157.

Fishwick S. & Reading A. M. 2008. Anomalous lithosphere beneath the Proterozoic of western and central Australia: a record of continental collision and intraplate deformation. *Precambrian Research* **166**, 111–121.

Fishwick S., Heintz M., Kennett B. L. N., Reading A. M. & Yoshizawa K. 2008. Steps in lithospheric thickness within eastern Australia, evidence from surface wave tomography. *Tectonics* **27**, doi:10.1029/2007TC002116.

Fishwick S., Kennett B. L. N. & Reading A. M. 2005. Contrasts in lithospheric structure within the Australian Craton—insights from surface wave tomography. *Earth and Planetary Science Letters* **231**, 163–176.

Ford H. A., Fischer K. M., Abt D. L., Rychert C. A. & Elkins-Tanton L. T. 2010. The lithosphere–asthenosphere boundary and cratonic lithospheric layering beneath Australia from Sp wave imaging. *Earth and Planetary Science Letters* **300**, 299–310.

Foster D. A. & Gray D. R. 2000. Evolution and structure of the Lachlan Fold Belt (Orogen) of eastern Australia. *Annual Reviews of Earth and Planetary Sciences* **28**, 47–80.

Glen R. A. 2005. The Tasmanides of eastern Australia. *In*: Vaughan A. P. M., Leat P. T. & Pankhurst R. J. eds. *Terrane processes at the margins of Gondwana*, pp. 23–96. *Geological Society*, London.

Goleby B. R., Blewett R. S., Fomin T., Fishwick S., Reading A. M., Henson P. A., Kennett B. L. N., Champion D. C., Jones L., Drummond B. J. & Nicoll M. 2006. An integrated multi-scale 3D seismic model of the Archaean Yilgarn Craton, Australia. *Tectonophysics* **420**, 75–90.

Gorbatov A. & Kennett B. L. N. 2003. Joint bulk-sound and shear tomography for Western Pacific subduction zones. *Earth and Planetary Science Letters* **210**, 527–543.

Graeber F. M., Houseman G. A. & Greenhalgh S. A. 2002. Regional teleseismic tomography of the western Lachlan Orogen and the Newer Volcanic Province, southeast Australia. *Geophysical Journal International* **149**, 249–266.

Graham S., Lambert D. D., Shee S. R., Smith C. B. & Reeves S. 1999. Re–Os isotopic evidence for Archaean lithospheric mantle beneath the Kimberley Block, Western Australia. *Geology* **27**, 431–434.

Handler M. & Bennett V. 2001. Constraining continental structure by integrating Os isotopic ages of lithospheric mantle with geophysical and crustal data: an example from southeastern Australia. *Tectonics* **20**, 177–188.

Jaques A. L. & Milligan P. R. 2004. Patterns and controls on the distribution of diamondiferous intrusions in Australia. *Lithos* **77**, 783–802.

Johnson R. W. Ed. 1989. *Intraplate volcanism: in eastern Australia and New Zealand*. Cambridge University Press, Cambridge, 432 pp.

Kaiho Y. & Kennett B. L. N. 2000. Three dimensional structure beneath the Australasian region from refracted wave observations. *Geophysical Journal International* **142**, 651–668.

Kennett B. L. N. 2003. Seismic structure in the mantle beneath Australia. *In*: Hillis R. R. & Müller R. D. eds. *Evolution and Dynamics of the Australian Plate*, pp. 7–23. Geological Society of Australia Special Publication **22** and Geological Society of America Special Paper 372.

Kennett B. L. N. & Abdullah A. 2011. Seismic wave attenuation beneath the Australasian region. *Australian Journal of Earth Sciences* **58**, 285–295.

Kennett B. L. N., Fishwick S. & Heintz M. 2004a. Lithospheric structure in the Australian region—a synthesis of surface and body wave studies. *Exploration Geophysics* **35**, 242–250.

Kennett B. L. N., Fishwick S., Reading A. M. & Rawlinson N. 2004b. Contrasts in mantle structure beneath Australia—Relation to Tasman Lines. *Australian Journal of Earth Sciences* **51**, 563–569.

Korsch R. J., Barton T. J., Gray D. R., Owen A. J. & Foster D. A. 2002. Geological interpretation of a deep seismic-reflection transect across the boundary between the Delamerian and Lachlan Orogens, in the vicinity of the Grampians, western Victoria. *Australian Journal of Earth Sciences* **49**, 1057–1075.

Lister G. S., Etheridge M. A. & Symonds P. A. 1986. Detachment faulting and the evolution of passive continental margins. *Geology* **14**, 246–250.

Moore W. B. & Schubert G. & Tackley P. 1998. Three-dimensional simulations of plume–lithosphere interaction at the Hawaiian Swell. *Science* **279**, 1008–1011.

Nataf H. & Ricard Y. 1996. An a priori tomographic model of the upper mantle based on geophysical modeling. *Physics of the Earth Planetary Interiors* **95**, 101–122.

O'Neill C. J., Moresi L. & Jaques A. L. 2005. Geodynamic controls on diamond deposits: implications for Australian occurrences. *Tectonophysics* **404**, 217–236.

Priestley K., McKenzie D., Debayle E. & Pilidou S. 2008. The African upper mantle and its relationship to tectonics and surface geology. *Geophysical Journal International* **175**, 1108–1126.

Rawlinson N. & Fishwick S. 2011. Seismic structure of the southeast Australian lithosphere from surface and body wave tomography. *Tectonophysics*, in press, doi:10.1016/j.tecto.2011.11.016.

Rawlinson N. & Kennett B. L. N. 2004. Rapid estimation of relative and absolute delay times across a network by adaptive stacking. *Geophysical Journal International* **157**, 332–340.

Rawlinson N. & Kennett B. L. N. 2008. Teleseismic tomography of the upper mantle beneath the southern Lachlan Orogen. *Physics of the Earth and Planetary Interiors* **167**, 84–97.

Rawlinson N. & Urvoy M. 2006. Simultaneous inversion of active and passive source datasets for 3-D seismic structure with application to Tasmania. *Geophysical Research Letters* **33**, doi:10.1029/2006GL028105.

Rawlinson N., Kennett B. L. N. & Heintz M. 2006b. Insights into the structure of the upper mantle beneath the Murray Basin from 3D teleseismic tomography. *Australian Journal of Earth Sciences* **53**, 595–604.

Rawlinson N., Kennett B. L. N., Vanacore E., Glen R. A. & Fishwick S. 2011. The structure of the upper mantle beneath the Delamerian and Lachlan orogens from simultaneous inversion of multiple teleseismic datasets. *Gondwana Research* **19**, 788–799.

Rawlinson N., Pozgay S. & Fishwick S. 2010b. Seismic tomography: A window into deep Earth. *Physics of the Earth and Planetary Interiors* **178**, 101–135.

Rawlinson N., Reading A. M. & Kennett B. L. N. 2006a. Lithospheric structure of Tasmania from a novel form of teleseismic tomography. *Journal of Geophysical Research* **111**, doi:10.1029/2005JB003803.

Rawlinson N., Tkalčić H. & Reading A. M. 2010a. Structure of the Tasmanian lithosphere from 3-D seismic tomography. *Australian Journal of Earth Sciences* **57**, 381–394.

Reading A. M., Kennett B. L. N. & Goleby B. 2007. New constraints on the seismic structure of West Australia: evidence for terrane stabilisation prior to the assembly of an ancient continent? *Geology* **35**, 379–382.

Reading A. M., Tkalčić H., Kennett B. L. N., Johnson S. P. & Sheppard S. 2012. Seismic structure of the crust and uppermost mantle of the Capricorn and Paterson Orogens and adjacent cratons, Western Australia, from passive seismic transects. *Precambrian Research* **196–197**, 295–308.

Schäfer J., Boschi L. & Kissling E. 2011. Adaptively parameterized surface wave tomography: methodology and a model of the European upper mantle. *Geophysical Journal International* **186**, 1431–1453.

Simons F. J. & van der Hilst R. D. 2002. Age-dependent seismic thickness and mechanical strength of the Australian lithosphere. *Geophysical Research Letters* **29**, doi:10.1029/2002GL014962.

Simons F. J., van der Hilst R. D., Montagner J-P. & Zielhuis A. 2002. Multimode Rayleigh wave inversion for heterogeneity and azimuthal anisotropy of the Australian upper mantle. *Geophysical Journal International* **151**, 738–754.

Simons F. J., Zielhuis A. & van der Hilst R. D. 1999. The deep structure of the Australian continent from surface wave tomography. *Lithos* **48**, 17–43.

van der Hilst R. D., Kennett B. L. N., Christie D. & Grant J. 1994. Project Skippy explores the mantle and lithosphere beneath Australia. *Transactions American Geophysical Union* **75**, 177.

Widiyantoro S. & van der Hilst R. D. 1996. Structure and evolution of lithospheric slab beneath the Sunda arc, Indonesia. *Science* **271**, 1566–1570.

Yoshizawa K. & Kennett B. L. N. 2004. Multimode surface wave tomography for the Australian region using a three-stage approach incorporating finite frequency effects. *Journal of Geophysical Research* **109**, doi:10.1029/2002JB002254.

Zielhuis A. & van der Hilst R. D. 1996. Upper-mantle shear velocity beneath eastern Australia from inversion of waveforms from SKIPPY portable arrays. *Geophysical Journal International* **127**, 1–16.

Received 26 October 2011; accepted 9 April 2012